

Evaluation of Spatially Targeted Scleral Stiffening on Neuroprotection in a Rat Model of Glaucoma

Brandon G. Gerberich^{1,*}, Bailey G. Hannon^{2,*}, Dillon M. Brown¹, A. Thomas Read¹, Matthew D. Ritch¹, Elisa Schrader Echeverri¹, Lauren Nichols³, Cahil Potnis⁴, Sreesh Sridhar¹, Maya G. Toothman⁵, Stephen A. Schwaner^{2,6}, Erin J. Winger³, Hannah Huang¹, Gabby S. Gershon¹, Andrew J. Feola^{1,4}, Mabelle T. Pardue^{1,4}, Mark R. Prausnitz^{1,3}, and C. Ross Ethier^{1,2}

¹ Wallace H. Coulter Department of Biomedical Engineering, Georgia Institute of Technology and Emory University, Atlanta, GA, USA

² George W. Woodruff School of Mechanical Engineering, Georgia Institute of Technology, Atlanta, GA, USA

³ School of Chemical and Biomolecular Engineering, Georgia Institute of Technology, Atlanta, GA, USA

⁴ Center for Visual and Neurocognitive Rehabilitation, Atlanta Veteran Affairs Healthcare System, Atlanta, GA, USA

⁵ College of Sciences, Georgia Institute of Technology, Atlanta, GA, USA

⁶ Exponent, Inc., Biomechanics Practice, Atlanta, GA, USA

Correspondence: C. Ross Ethier, Georgia Institute of Technology and Emory University, 315 Ferst Dr NW, Atlanta, GA 30332, USA. e-mail: ross.ethier@bme.gatech.edu

Received: December 31, 2021

Accepted: March 14, 2022

Published: May 10, 2022

Keywords: sclera; biomechanics; glaucoma; retinal ganglion cells

Citation: Gerberich BG, Hannon BG, Brown DM, Read AT, Ritch MD, Schrader Echeverri E, Nichols L, Potnis C, Sridhar S, Toothman MG, Schwaner SA, Winger EJ, Huang H, Gershon GS, Feola AJ, Pardue MT, Prausnitz MR, Ethier CR. Evaluation of spatially targeted scleral stiffening on neuroprotection in a rat model of glaucoma. *Transl Vis Sci Technol.* 2022;11(5):7. <https://doi.org/10.1167/tvst.11.5.7>

Purpose: Scleral stiffening may protect against glaucomatous retinal ganglion cell (RGC) loss or dysfunction associated with ocular hypertension. Here, we assess the potential neuroprotective effects of two treatments designed to stiffen either the entire posterior sclera or only the sclera adjacent to the peripapillary sclera in an experimental model of glaucoma.

Methods: Rat sclerae were stiffened in vivo using either genipin (crosslinking the entire posterior sclera) or a regionally selective photosensitizer, methylene blue (stiffening only the juxtaperipapillary region surrounding the optic nerve). Ocular hypertension was induced using magnetic microbeads delivered to the anterior chamber. Morphological and functional outcomes, including optic nerve axon count and appearance, retinal thickness measured by optical coherence tomography, optomotor response, and electroretinography traces, were assessed.

Results: Both local (juxtaperipapillary) and global (whole posterior) scleral stiffening treatments were successful at increasing scleral stiffness, but neither provided demonstrable neuroprotection in hypertensive eyes as assessed by RGC axon counts and appearance, optomotor response, or electroretinography. There was a weak indication that scleral crosslinking protected against retinal thinning as assessed by optical coherence tomography.

Conclusions: Scleral stiffening was not demonstrated to be neuroprotective in ocular hypertensive rats. We hypothesize that the absence of benefit may in part be due to RGC loss associated with the scleral stiffening agents themselves (mild in the case of genipin, and moderate in the case of methylene blue), negating any potential benefit of scleral stiffening.

Translational Relevance: The development of scleral stiffening as a neuroprotective treatment will require the identification of better tolerated stiffening protocols and further preclinical testing.

Introduction

Glaucoma is the leading cause of irreversible blindness, affecting nearly 80 million people worldwide.¹ This optic neuropathy is characterized by loss of retinal ganglion cell (RGC) axons in the optic nerve head (ONH), which is a main and early site of damage.² Because the only currently modifiable risk factor for glaucoma is the intraocular pressure (IOP), all current treatments aim to lower the IOP.^{3–5} However, such treatments are not always effective, and medication-based treatments have poor patient compliance.^{6,7} Therefore, additional treatment approaches are desired.

An elevated IOP leads to increased biomechanical strain in the ONH, which is thought to promote RGC damage and loss.⁸ We and others have proposed that biomechanical interventions could protect against this IOP-induced mechanical insult at the ONH,² with finite element modelling studies suggesting that scleral stiffening would have the greatest impact on decreasing ONH mechanical strains.^{9,10} Coudrillier et al.¹¹ experimentally verified that local peripapillary scleral stiffening reduced ONH biomechanical strain in ex vivo porcine eyes.

Kimball et al.¹² assessed glaucomatous damage in mice after stiffening the sclera using glyceraldehyde, a collagen crosslinking agent. Unexpectedly, scleral stiffening increased rather than decreased glaucomatous damage. One possible explanation of this result is that stiffening the entire sclera increased the magnitude of IOP fluctuations,¹³ in turn exacerbating RGC axonal damage.¹⁴ This result motivates the development of a spatially targeted stiffening approach.

To further investigate the neuroprotective potential of scleral stiffening, we thus considered two different stiffening approaches (Supplementary Table S1). In the first, we selectively stiffened only the juxtaperipapillary sclera (adjacent to the peripapillary sclera) using the photosensitizer methylene blue (MB) in combination with selective laser illumination of a thin annulus surrounding the ONH. In this way, we hypothesized that localized juxtaperipapillary stiffening would prevent glaucomatous damage by decreasing ONH biomechanical strain without broadly changing the overall compliance of the globe and thus maintain a normal ocular pulse amplitude. Our second approach was to stiffen the entire posterior sclera using a well-tolerated collagen crosslinking agent, genipin (GP), which has a promising safety profile^{15–18} and has recently been shown to provide sustained scleral stiffening at a much lower concentration than glyceraldehyde^{19,20} while preserving retinal function.²¹ We assess

the protective effects of these two stiffening paradigms in a rodent model of ocular hypertension (OHT).

Methods

Study Design

We chose the Brown Norway rat model of glaucoma because it is widely used, demonstrates several of the clinical hallmarks of glaucoma, and these animals are docile enough to accurately measure IOP without the use of anesthesia.^{22–25} In this study, 86 male, retired breeder Brown Norway rats (8–10 months old) were purchased from Charles River Laboratories (Wilmington, MA). All procedures involving animals were approved by the Georgia Institute of Technology and the Atlanta VA Healthcare System Institutional Animal Care and Use Committees, and complied with the ARVO statement for the Use of Animals in Ophthalmic and Vision Research.

Rats were divided randomly into three treatment groups (Fig. 1A) to receive one of three unilateral treatments: (i) sham, (ii) whole posterior scleral stiffening, or (iii) juxtaperipapillary scleral stiffening. Within each animal, the eye receiving treatment was randomly assigned (left or right). Hanks balanced salt solution (HBSS) was used as the vehicle for stiffening treatments and as the sham treatment. In brief, the negative (sham) control group (HBSS rats, $n = 32$) received a retrobulbar injection of HBSS (150 μ L). The second group (GP rats, $n = 27$) received 15 mM GP by retrobulbar injection (150 μ L) to induce chemical crosslinking of the whole posterior sclera. The third group (MB rats, $n = 27$) received 3 mM MB by retrobulbar injection (100 μ L), followed by targeted transpupillary light delivery to photocrosslink the juxtaperipapillary sclera. Previously published studies^{19–21,26} have evaluated the toxicity and efficacy of these stiffening treatments. For the MB-treated eyes, light was targeted to an annular region of 1 mm inner diameter and 2 mm outer diameter, equating approximately to subtended half-angles of 4.5° (inner edge) and 9° (outer edge), assuming an axial length of 6.5 mm.²⁷ This corresponds approximately with the peripheral sclera region of Fazio et al.²⁸ and a mix of regions R1 and R2 of Cone-Kimball et al.²⁹ Here, we call this the “juxtaperipapillary sclera.” More details of this photocrosslinking procedure are described in the Supplementary Material (Supplementary Fig. S2).

Seven days after scleral stiffening, OHT was induced by injection of magnetic microbeads into the anterior chamber of stiffened eyes (discussed elsewhere in this article), creating three cohorts of eyes: HBSS

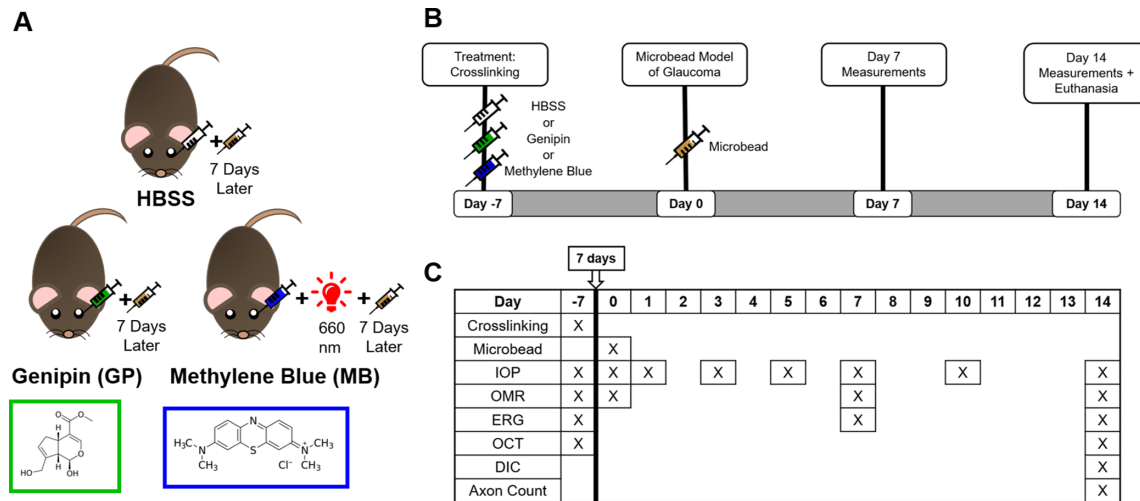


Figure 1. Experimental design of the study. **(A)** An overview of the experimental approach, showing scleral crosslinked eyes receiving one of three treatments by retrobulbar injection: HBSS (sham vehicle), GP, or MB. Those in the MB group also received 30 minutes of localized red light (660 nm) to selectively stiffen the juxtaperipapillary (but not peripheral) sclera. **(B)** Timeline of experiments. Seven days after scleral stiffening treatment, the treated (“experimental”) eye received a microbead injection to induce OHT. Taking the date of OHT induction as day 0, rats were sacrificed at day 14. **(C)** Timing of experiments. IOP measurements were taken at days -7 , 0 , 1 , 3 , 4 , 7 , 10 , and 14 . OMR measurements were taken at days 0 , 7 , and 14 . ERG measurements were taken at days -7 , 7 , and 14 , and OCT images were acquired at days -7 and 14 . DIC and axon count measurements were taken by collecting the sclerae and optic nerves on day 14 immediately after euthanasia.

hypertensive experimental eyes in HBSS rats, GP hypertensive experimental eyes in GP rats, and MB hypertensive experimental eyes in MB rats (Fig. 1B). Contralateral eyes received no injections and therefore served as normotensive controls for each animal (HBSS normotensive control eyes, GP normotensive control eyes, and MB normotensive control eyes). The rationale for this unpaired experimental design is described in the Supplementary Material (Supplementary Table S2, Supplementary Fig. S1). We considered multiple outcome measures: IOP, electroretinography (ERG), optomotor response (OMR), optical coherence tomography (OCT) imaging of the retina, optic nerve axon counts, ocular globe size measurements, and scleral stiffness (biomechanical measurements). The total numbers of eyes analyzed for each outcome measure are reported in Supplementary Table S3.

Microbead Model of Glaucoma

The magnetic microbead model of glaucoma^{30,31} was used to induce unilateral OHT in eyes designated as hypertensive experimental. All microbead injections occurred at day 0, which was seven days after scleral crosslinking (Fig. 1B). Rats were euthanized 14 days after induction of OHT. A 25 μ L volume of 2 μ m and 6 μ m (1:1) magnetic polystyrene microbeads (micromer-M, Micromod, Rostock, Germany) suspended in HBSS was used for microbead injections, as described fully in the Supplementary Material.

IOP Measurements and IOP Burden Calculation

IOP measurements were taken in awake rats using a tonometer (Icare TONOLAB, Vantaa, Finland) at baseline and days 0 , 1 , 3 , 5 , 7 , 10 , and 14 after microbead injection (Fig. 1C). If the experimental (injected) eye did not demonstrate at least 1 day of OHT, defined as an IOP elevation of more than 5 mm Hg compared with the contralateral control eye within 7 days of injection, the eye was considered to be a nonresponder and was then reinjected with 15 μ L of microbead solution on day 7 ($n = 12$ of 74 total rats). Rats for which IOP elevation failed 7 days after reinjection were removed from the study ($n = 3$); therefore, no rat was reinjected with microbeads more than once. From IOP measurements we also calculated an IOP burden, which provides an estimate of the total IOP insult to the hypertensive eye. IOP burden is sometimes referred to as the cumulative IOP difference,³² IOP exposure,³³ or positive integral IOP.³⁴ We defined IOP burden as the area between the OHT and normotensive eyes on the IOP versus time plot (see Supplementary Material).

Assessment of Retinal and Visual Function: ERG and OMR

Dark-adapted ERGs were used to assess inner and outer retinal neuronal function (see Supplementary Materials). ERG measurements were taken at

baseline (before the crosslinking procedure), and at 7 and 14 days after microbead injection (Fig. 1C). We analyzed amplitudes of the positive scotopic threshold and negative scotopic threshold signals at $-6.0 \log \text{cd s/m}^2$, the b-wave at $-3.0 \log \text{cd s/m}^2$ (b-wave), and the third oscillatory potential (OP3) at $2.1 \log \text{cd s/m}^2$, because these amplitudes have been shown to be significantly decreased in rodent models of glaucoma.^{35–39}

Visual function was assessed via quantitative analysis of OMR thresholds of spatial frequency and contrast sensitivity (CS) (see Supplementary Materials, OptoMotry; Cerebral-Mechanics, Lethbridge, AB, Canada). The OMR was measured at baseline (before crosslinking treatment), day 0 (7 days after crosslinking procedure, but before microbead injection that day), day 7, and day 14 (Fig. 1C), following a protocol similar to that of Prusky et al. and Douglas et al.^{40,41}

ERG-based Ischemic Damage Exclusion Criteria

Rats with likely ischemic damage to the retina were excluded from analysis using an ERG-based (and not IOP-based) exclusion criterion.^{42,43} In brief, exclusion was based on the b-wave amplitude from the brightest flash ($2.1 \log \text{cd s/m}^2$) ERG at day 14, because bipolar cell function (which drives b-wave amplitude) is known to be sensitive to ischemic damage at bright scotopic flashes.^{44,45} The 99.5% confidence interval of the b-wave amplitude was computed for all normotensive control eyes ($n = 74$). If the b-wave amplitude of the hypertensive experimental eye lay below this 99.5% confidence interval, that rat was excluded from analysis. Of the 74 rats analyzed, 14 rats were excluded by this criterion, leaving 60 rats included in the final analysis (Supplementary Table S3).

Assessment of RGCs: OCT and Axon Counts

A spectral domain OCT system (Bioptigen 4300, Leica Microsystems, Buffalo Grove, IL) was used to measure total retinal thickness (TRT) and to qualitatively assess retinal morphology in the posterior eye at baseline (day -7 , before retrobulbar injection) and day 14 (Fig. 1C) in a similar manner to method previously reported.⁴⁶ TRT was measured at locations 0.5 mm and 1.2 mm from the center of the ONH (see Supplementary Material).

Immediately after euthanasia via CO_2 overdose at day 14 (Fig. 1C), optic nerves were dissected from enucleated eyes and prepared for histology (see Supplementary Material). Normal-appearing RGC axons were counted automatically from histological cross-sections of the entire optic nerve using AxoNet, a fully

convolutional neural network previously developed in our laboratory.^{47,48} Histological images of the optic nerves were also graded by six trained graders using an existing semiquantitative grading scheme.^{49,50} All six trained graders individually assigned a score ranging from 1 (healthy) to 5 (extremely damaged) to each optic nerve image and these scores were then averaged to obtain a single grade for each nerve.

We did not undertake RGC counts in addition to axon counts for several reasons. First, we judged it very important to measure scleral stiffness at the end of the experiment, and were concerned that removal of the retina could have affected our scleral DIC stiffness measurements. Second, counting of retinal RGC soma can miss axonal loss due to the Wallerian nature of axon die-back in glaucoma, in which soma can transiently persist after axonal loss. Considering the rapid time course of our glaucoma model, this was a significant concern.

Assessment of Eye Size

Upon enucleation, excess tissue was removed with micro scissors, leaving the globe intact with optic nerve. Eyes were then placed superior quadrant upwards with the optical axis parallel to the imaging surface, and an iPhone 8 (Apple Inc, Cupertino, CA) camera was used to image from above. Axial length (defined here as anterior corneal surface to scleral canal), equatorial width (widest nasal–temporal width), and anterior chamber depth (anterior corneal surface to limbus along optical axis) were determined using ImageJ software⁵¹ calibrated with a reference scale object in all images.

Whole Globe Inflation Testing

After trimming the optic nerve for RGC axon counting, eyes underwent whole globe inflation testing as previously described²⁰ to verify scleral stiffening at day 14 (Fig. 1C). The dura was left intact during inflation testing to avoid leakage of fluid from the scleral canal. Therefore, we could not measure strains in the scleral region that was optically obstructed by the dura and blood vessels, and reported strains are from regions with optical access during DIC (digital image correlation) measurements. Several modifications to the previously published method were made to adapt to the altered mechanical properties of microbead-injected eyes (see Supplementary Material).

We also considered characterizing scleral stiffness by atomic force microscopy (AFM), but ultimately chose not to for several reasons. First, AFM gives very local measurements and thus requires that many locations be

interrogated to obtain a measure of overall scleral stiffness. Second, and more important, AFM applies a local through-plane compressive load to sclera, which is not the main mode of loading due to ocular hypertension. This is in distinction to our inflation tests, which interrogated a mode of loading which is highly relevant to the hypertensive eye.

Data Analysis

Data were analyzed using GraphPad Prism software (GraphPad Prism Software 8.2.1, San Diego, CA) and R (R Core Team, 2020) 3.6.3 software, and all data were graphed using GraphPad Prism. Analysis of IOP was performed using a repeated measures two-way analysis of variance (ANOVA) (fixed factors: time, treatment group; random factor: rat ID) with Tukey post hoc tests for changes in IOP over time and one-way ANOVA for differences in IOP burden between treatment groups using GraphPad Prism. Scleral strain was assessed using a two-way repeated measures ANOVA (fixed factors: treatment group, strain location; random factor: rat ID) and post hoc comparisons were alpha corrected using the multivariate t method in R. Full statistical analyses are presented in detail in Supplementary Material.

Results

Mechanical Testing Confirmed That Crosslinking Increased Scleral Stiffness

Stiffening of the entire posterior sclera by GP and of just the juxtaperipapillary sclera by MB was successful, as confirmed by whole globe inflation of enucleated eyes 14 days after induction of OHT (Fig. 2). We observed a differential effect on scleral stiffening depending on the type of treatment and measurement location, that is, there was a significant interaction effect between the treatment and the location, 2-way repeated measures ANOVA, $F(5,105.91) = 9.6382$, $P < 0.0001$. Specifically, mean scleral strain was two- to three-fold lower (i.e., stiffness was greater) in both the peripheral and juxtaperipapillary scleral regions in GP eyes compared with the corresponding regions in HBSS eyes (Fig. 2B) ($P < 0.0001$ for both), indicating successful whole posterior scleral crosslinking. There was no significant difference in scleral strains between the peripheral and juxtaperipapillary regions within GP eyes ($P = 0.6809$).

In MB eyes, juxtaperipapillary scleral strain was approximately three-fold lower than in HBSS-treated eyes (Fig. 2B) ($P < 0.0001$), whereas peripheral strains

did not differ significantly between HBSS and MB eyes ($P = 0.5316$), indicating targeted crosslinking of the juxtaperipapillary sclera. Furthermore, MB eyes had significantly reduced strain in the juxtaperipapillary region compared with the peripheral region within the same MB eye (Fig. 2B, $P = 0.0002$), further indicating successfully targeted stiffening. We conclude that both GP and MB were efficacious in stiffening the sclera for at least 2 weeks, and that targeted juxtaperipapillary scleral stiffening with photoactivated MB is feasible.

Microbead Injection Successfully Increased IOP and Led to Increased Globe Size

Microbead treatment at day 0 produced an IOP elevation with an initial rapid rise peaking at day 3, followed by a gradual decrease until sacrifice at day 14 (Fig. 2D). At all time points after microbead injection, the mean IOP in microbead eyes was significantly elevated compared with normotensive controls (Fig. 2D), two-way repeated measures ANOVA, Time \times Treatment: $F(30, 684) = 8.716$, $P < 0.0001$, Tukey post hoc test, except for the GP cohort at day 14. No significant differences in IOP were found between microbead treatment groups at any time point (Fig. 2D) (all $P > 0.05$). The mean IOP burden also did not differ between microbead treatment groups (Fig. 2C), one-way ANOVA, $F(2, 57) = 1.629$, $P = 0.21$.

We also observed that hypertensive eyes were significantly larger than normotensive control eyes for all three treatment groups, as measured by axial length, equatorial width, and anterior chamber depth (Fig. 3) (all $P < 0.0001$; compare data points from hypertensive eyes with grey shaded region representing normotensive eyes), consistent with known effects of extended exposure to elevated IOP.^{12,32} No significant differences in eye size were found between GP and MB scleral stiffening treatment groups in hypertensive eyes.

RGC Axons Were Not Preserved by Scleral Stiffening

As expected, RGC axons were lost owing to OHT, with greater IOP burdens associated with lower optic nerve axon counts and poorer axonal appearance (Supplementary Table S5) ($P < 0.0001$), and representative optic nerve images (Supplementary Fig. S5). Also as expected, axon counts and nerve grades were closely correlated with one another (Supplementary Fig. S7) (all $P < 0.0001$). However, scleral stiffening by either GP or MB in hypertensive eyes was not found to significantly preserve RGC axons (Table, Supplementary Table S6, and Figs. 4A and B).

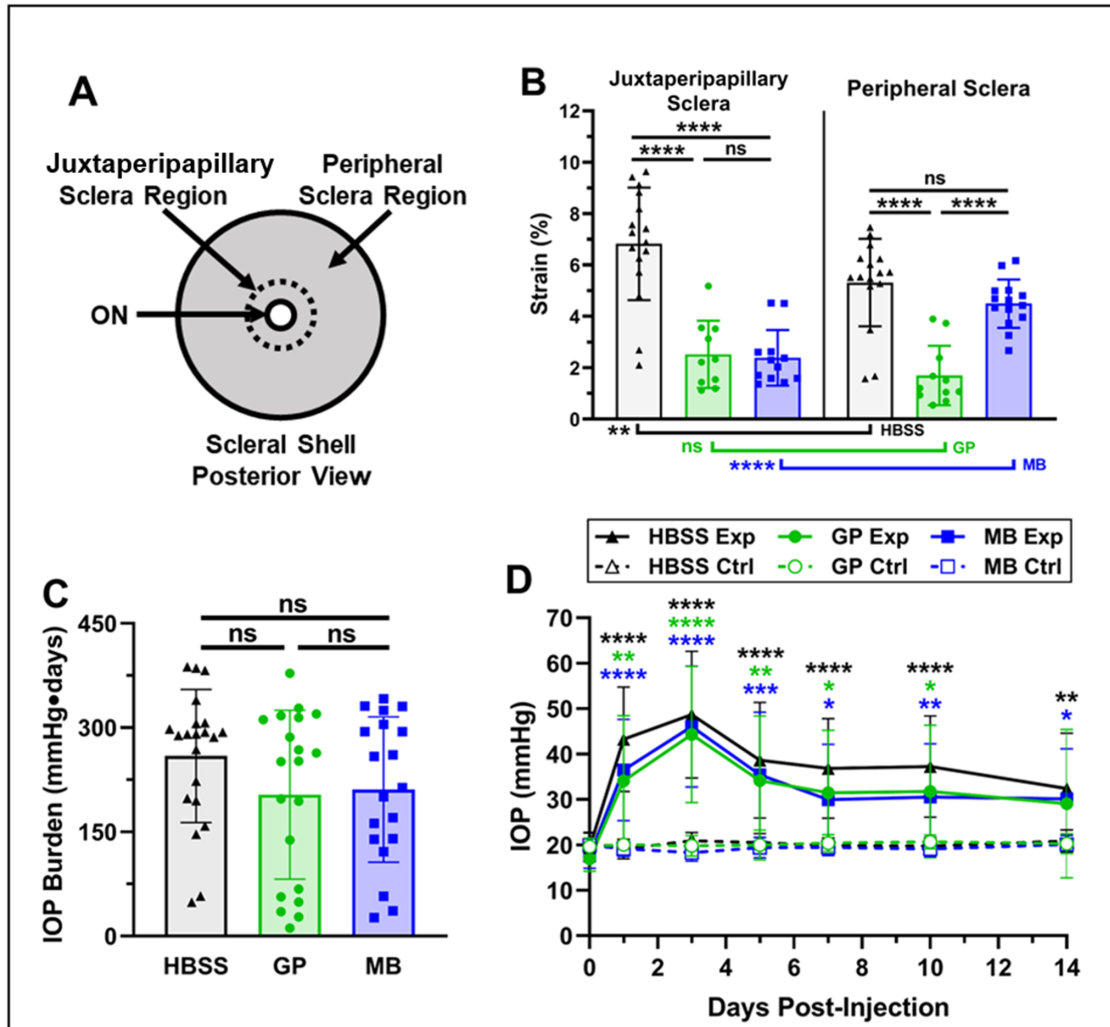


Figure 2. GP and MB significantly increased scleral stiffness in OHT eyes. **(A)** Representation of the posterior eye showing the juxtaperipapillary sclera, here defined as the region enclosed by a 2-mm diameter circle centered at the ON. The peripheral sclera was defined as the sclera outside this region. **(B)** Whole globe inflation testing showed that posterior scleral stiffening with GP and targeted juxtaperipapillary sclera stiffening with MB were effective. The reported values are the mean strains over the juxtaperipapillary and peripheral scleral regions, a quantity that is inversely proportional to scleral stiffness. **(C)** IOP burden did not differ significantly between treatment groups. **(D)** IOP increased after induction of OHT at day 0 in microbead-injected eyes compared with normotensive control eyes. Statistical significance is indicated as: * $P < 0.05$, ** $P < 0.01$, *** $P < 0.001$, and **** $P < 0.0001$. Data shown as mean \pm standard deviation. DIC = digital image correlation.

Consistent with these observations, additional analysis of axonal density (axons/area) and optic nerve cross-sectional area (Supplementary Fig. S6) showed a significant decrease in axonal density with increased IOP burden in hypertensive eyes vs. normotensive eyes, but revealed no significant protective effect of scleral stiffening in hypertensive eyes (Table, Supplementary Table S6, and Supplementary Fig. S4) ($P < 0.0001$). These results reveal that both juxtaperipapillary (MB) and whole posterior (GP) stiffening treatments did not protect against RGC axonal loss, but also did not increase RGC axonal loss when compared with sham treated eyes. Importantly, in prior studies (Gerberich et al.²⁶; Hannon et al.²¹), we observed axonal loss

owing to scleral stiffening alone, with mean RGC axon counts of 74,000, 68,000, and 46,000 for HBSS-, GP-, and MB-treated eyes, respectively; we discuss the implications of this previous finding elsewhere in this article.

Retinal Thickness Measurements Were Inconclusive Regarding a Protective Effect of Scleral Stiffening

RGC axonal loss can decrease TRT. We used OCT to measure TRT at two locations (0.5 mm and 1.2 mm from the ONH) (Figs. 4C and D). However, at 0.5 mm from the ONH we did not observe a

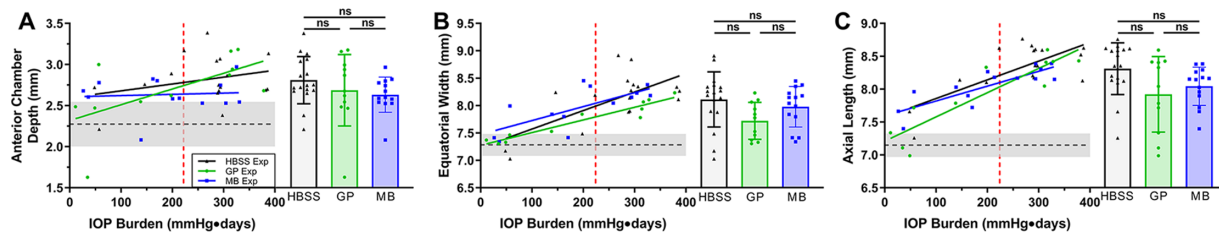


Figure 3. OHT-induced globe enlargement. (A) Anterior chamber depth, (B) equatorial width, and (C) axial length were quantified versus IOP burden. It is interesting and perhaps unexpected that crosslinked eyes showed axial elongation (Fig. 3C); we speculate that this was due to corneal remodeling and perhaps some scleral remodeling in cross-linked sclerae. In this and subsequent graphs, the left side shows a plot of the outcome measure versus IOP burden at day 14, with raw data and linear regressions for each scleral stiffening treatment group shown. Dashed horizontal lines and grey bands represent the mean values and corresponding standard deviations from normotensive control eyes. The dashed red vertical line shows the mean IOP burden as reported in Supplementary Table S3. The right shows data corrected to this mean IOP burden by the statistical analysis. Statistical significance is judged by differences at the mean IOP burden as reported in Supplementary Table S3. Significance of slopes and comparisons with each group are listed in Supplementary Table S4. Data shown as mean ± standard deviation. Ctrl = control; Exp = experimental; ns = not significant.

Table. Adjusted Means and Simple Comparisons for Each Parameter Measured From Rat Microbead Study

Outcome Parameter	Day	Value at Mean IOP Burden						Comparisons					
		Normotensive Eye			Hypertensive Eye			Between Hypertensive Eyes			Normotensive vs Hypertensive		
		HBSS	GP	MB	HBSS	GP	MB	HBSS-GP	HBSS-MB	GP-MB	HBSS	GP	MB
Juxtapapillary Strain (%)	14	3.79	2.77	3.07	6.18	2.52	2.59	<0.0001	<0.0001	1.0000	<0.0001	0.9891	0.7234
Peripheral Strain (%)	14	2.62	2.10	2.20	4.83	1.84	4.55	<0.0001	0.9446	<0.0001	<0.0001	0.9035	<0.0001
Equatorial Diameter (mm)	14	7.3	7.30	7.24	7.99	7.79	8.05	0.2135	0.9765	0.0734	<0.0001	<0.0001	<0.0001
Axial Length (mm)	14	7.18	7.16	7.10	8.22	8.04	8.11	0.1796	0.5991	0.9147	<0.0001	<0.0001	<0.0001
Anterior Chamber Depth (mm)	14	2.34	2.29	2.13	2.79	2.70	2.67	0.9239	0.7704	0.9996	<0.0001	<0.0001	<0.0001
Nerve Cross-sectional Area (mm ²)	14	0.262	0.259	0.285	0.250	0.270	0.277	0.7233	0.455	0.9963	0.9566	0.9621	0.9915
Axon Count (Axons)	14	79,083	78,003	78,597	35,884	42,042	41,288	0.6302	0.7152	0.9999	<0.0001	<0.0001	<0.0001
Nerve Grade (AU)	14	1.32	1.23	1.43	3.76	3.45	3.66	0.4762	0.9885	0.7872	<0.0001	<0.0001	<0.0001
Axon Density (Axons/mm ²)	14	289,520	301,906	279,214	136,346	152,371	147,867	0.8832	0.9623	0.9995	<0.0001	<0.0001	<0.0001
Retinal Thickness at 0.5mm (mm)	14	0.211	0.208	0.206	0.186	0.198	0.164	0.4618	0.0270	0.0002	0.0098	0.6384	<0.0001
Retinal Thickness at 1.2mm (mm)	14	0.193	0.189	0.193	0.181	0.192	0.187	0.0116	0.3443	0.5861	0.0033	0.8455	0.4308
Contrast Sensitivity (AU) ^a	7				2.33	2.24	2.22	0.7604	0.9987	0.984	<0.0001	<0.0001	<0.0001
	14	5.43	5.61	5.80	2.33	1.81	2.12	1.0000	1.0000	1.0000	<0.0001	<0.0001	<0.0001
Spatial Frequency (c/d) ^a	7				0.331	0.298	0.313	0.7664	0.9780	0.9993	<0.0001	<0.0001	<0.0001
	14	0.574	0.571	0.577	0.328	0.282	0.304	0.5741	0.9770	0.9875	<0.0001	<0.0001	<0.0001
pSTR Amplitude (μV)	7	8.67	10.35	8.09	2.61	3.14	1.93	0.9826	0.9479	0.6312	<0.0001	<0.0001	<0.0001
	14	6.62	7.38	8.89	2.18	2.05	1.6	0.9999	0.9131	0.9686	<0.0001	<0.0001	<0.0001
nSTR Amplitude (μV)	7	7.38	8.42	7.89	5.94	4.63	4.13	0.6174	0.2706	0.9904	0.3512	<0.0001	<0.0001
	14	6.86	7.99	8.14	4.61	3.84	4.15	0.8238	0.9773	0.9952	0.0044	<0.0001	<0.0001
B-wave Amplitude (μV)	7	248.7	304.1	238.0	130.6	149.8	80.6	0.9423	0.2001	0.0256	<0.0001	<0.0001	<0.0001
	14	224.3	248.9	272.9	109.5	103.8	92.1	0.9999	0.8854	0.9745	<0.0001	<0.0001	<0.0001
OP3 Amplitude (μV)	7	86.5	96.8	78.9	45.1	62.7	56.4	0.0180	0.2700	0.8392	0.0018	<0.0001	<0.0001
	14	79.6	84.4	90.2	45.1	42	46.2	0.9898	0.9999	0.9635	<0.0001	<0.0001	<0.0001

Significant *P*-values are colored in green; highly significant (*P* < 0.0001) *P*-values are bolded.

^aNormotensive eye values are at baseline timepoint, and not at day 7 or 14. AU = arbitrary units. pSTR = positive scotopic threshold; nSTR = negative scotopic threshold.

significant protective effect of scleral stiffening when examining TRT. Specifically, TRT was not significantly different between GP and HBSS hypertensive eyes (Table, Supplementary Table S6, and Fig. 4C), and was decreased in MB eyes compared with HBSS eyes (*P* = 0.027) (Table) and GP eyes (*P* = 0.0002) (Table). TRT at 0.5 mm from the ONH was significantly less in hypertensive experimental eyes for both HBSS (*P* = 0.0098) and MB (*P* < 0.0001) cohorts compared with

their respective normotensive controls, but not for GP eyes (Table, Fig. 4C).

At 1.2 mm from the ONH, hypertensive HBSS eyes showed significantly decreased TRT compared with GP eyes (Table and Supplementary Table S6) mean ± standard error, 0.181 ± 0.00244 mm vs. 0.192 ± 0.0025 mm; *P* = 0.0116), potentially indicating a protective effect of GP against retinal changes (Fig. 4C); however, no significant differences were observed in this measure

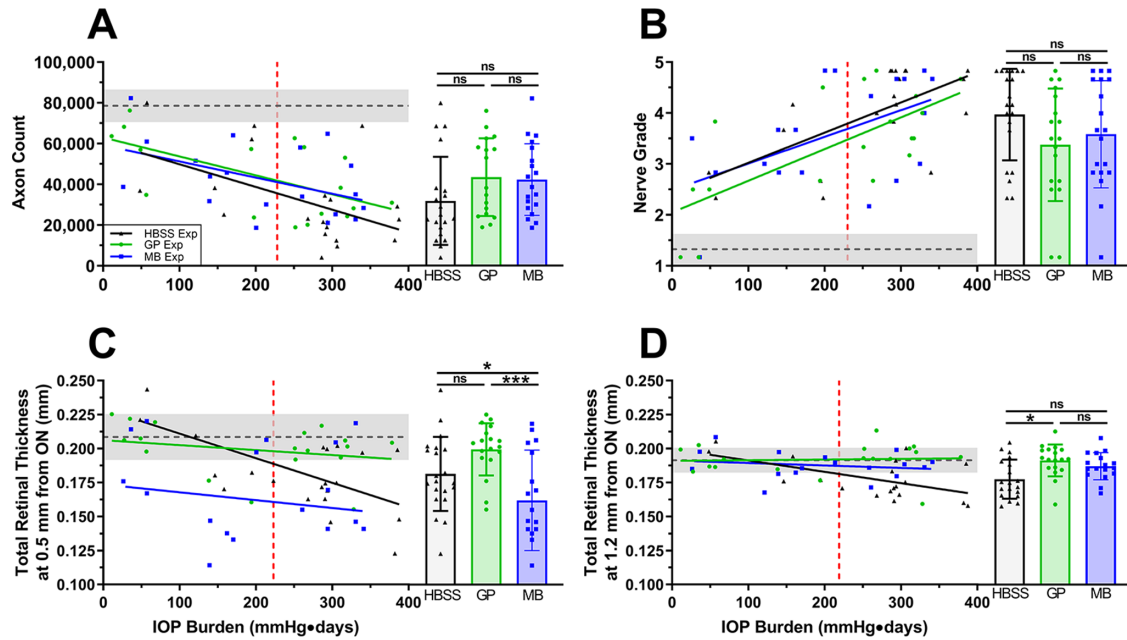


Figure 4. The number of RGCs and TRT did not demonstrably benefit from scleral stiffening treatments. **(A)** Whole nerve axon counts for hypertensive experimental eyes. **(B)** Nerve gradings (on a scale of 1 to 5; 1 being a healthy nerve and 5 being a highly damaged nerve) for hypertensive experimental ONs. Both analyses reported in **(A)** and **(B)** showed no significant protective effects of crosslinking. **(C)** TRT measured 0.5 mm from the ONH versus IOP burden. Retinal thickness in hypertensive GP eyes was not different than in GP normotensive controls, while thickness in hypertensive HBSS eyes was significantly less than in HBSS normotensive controls. Thickness in hypertensive MB eyes was less than in hypertensive GP and HBSS eyes (* indicates $P = 0.027$, *** indicates $P = 0.0002$). **(D)** TRT measured 1.2 mm from the ONH. Thicknesses in both GP- and MB-treated hypertensive eyes were not significantly different from their respective normotensive contralateral control eye thicknesses, whereas thickness in hypertensive HBSS-treated eyes was significantly less than in HBSS normotensive control eyes. Thickness in hypertensive GP eyes was significantly greater than in hypertensive HBSS-treated eyes (* $P = 0.01$). Significance of slopes and comparisons with each group are listed in Supplementary Table S4. See legend for Fig. 3 for interpretation of graphs. ns = not significant. Data shown as mean \pm standard deviation.

of TRT between hypertensive GP eyes and MB eyes or between hypertensive MB eyes and HBSS eyes. As expected, TRT was significantly lower in hypertensive HBSS eyes when compared with their normotensive controls (Table and Supplementary Table S6) (mean \pm standard error, 0.181 ± 0.00244 mm vs 0.193 ± 0.00232 mm; $P < 0.0001$); interestingly, such a difference was not noted between hypertensive and normotensive eyes for GP- or MB-treated eyes. Representative OCT images shown in Supplementary Fig. S4 reveal minor qualitative differences between treatment groups as well as indications of characteristic glaucomatous cupping at higher IOP burdens.

Examination of slopes in Figs. 4C and D (Supplementary Table S4) suggest a trend (not reaching statistical significance) of less dependence of TRT on IOP burden after scleral stiffening both at 0.5 mm from the ONH (GP: $P = 0.559$; MB: $P = 0.769$) and 1.2 mm from the ONH (GP: $P = 0.986$; MB: $P = 0.872$), whereas there is a significant slope in HBSS hypertensive eyes at both 0.5 mm ($P = 0.0141$) and 1.2 mm ($P = 0.0039$) from the ONH. These results indicate a slight preservation of TRT in GP-treated hypertensive eyes.

Visual Outcomes and RGC Function Were Not Preserved by Scleral Stiffening

In addition to structural measures, we assessed visual function by OMR and ERG. The mean values of CS and spatial frequency thresholds measured by OMR were significantly decreased at days 7 and 14 in hypertensive experimental eyes when compared with their baseline values for all three treatment groups (Table) ($P < 0.0001$). The mean values for each at both time points were not found to differ between treatment groups in hypertensive eyes (Fig. 5, Table) ($P > 0.05$). Both measures of visual function were found to vary with the degree of IOP burden (Supplementary Table S5) ($P < 0.0001$); however, for CS, this relationship varied depending on the scleral stiffening treatment (Supplementary Table S5) ($P = 0.011$). Comparisons of slopes (outcome measures vs. IOP burden) showed that CS of the MB group did not vary with IOP burden ($P = 0.99$).

ERG measurements showed no significant differences in the mean positive scotopic threshold, negative scotopic threshold, b-wave, or OP amplitudes between

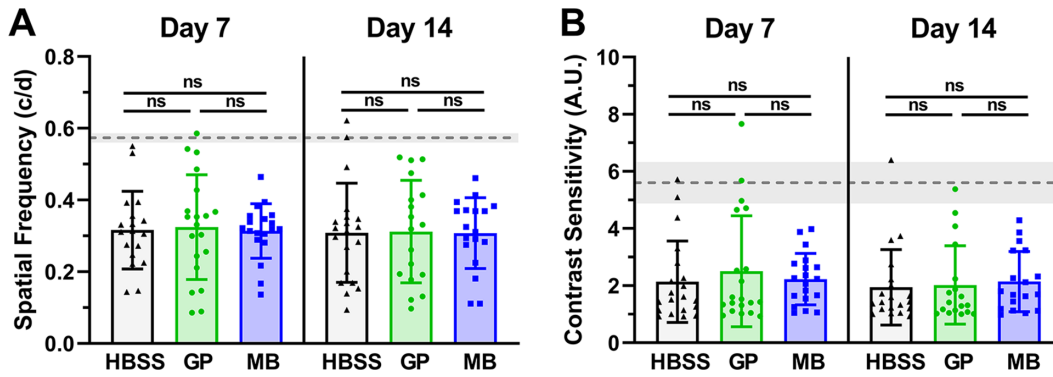


Figure 5. Visual function was unchanged by scleral stiffening treatment. (A) Spatial frequency thresholds and (B) CS thresholds at days 7 and 14 for hypertensive experimental eyes. All plotted quantities are corrected to the mean IOP burden at either day 7 or 14, as appropriate, as described in Fig. 3. In this figure, the dashed lines and grey bands represent mean values and their corresponding standard deviations from baseline hypertensive experimental eyes (owing to hyperacuity of control eyes, Supplementary Fig. S3). Significance of comparisons are listed in Supplementary Table S4. ns = not significant. Data shown as mean ± standard deviation.

any treatment group in hypertensive eyes at day 7 or day 14 after OHT induction (Table, Supplementary Table S6, and Fig. 6). Significant decreases in these outcomes were observed in hypertensive experimental eyes compared with normotensive control eyes for all three treatment groups (Table) ($P < 0.01$). The positive

scotopic threshold, b-wave, and OP3 amplitudes were significantly affected by IOP burden (Supplementary Table S5) ($P < 0.01$). The slope of these relationships (outcome measure vs. IOP burden) varied with treatment in the case of b-wave (bead:treatment:IOP burden) ($P = 0.0221$) and OP3 ($P = 0.0461$). The

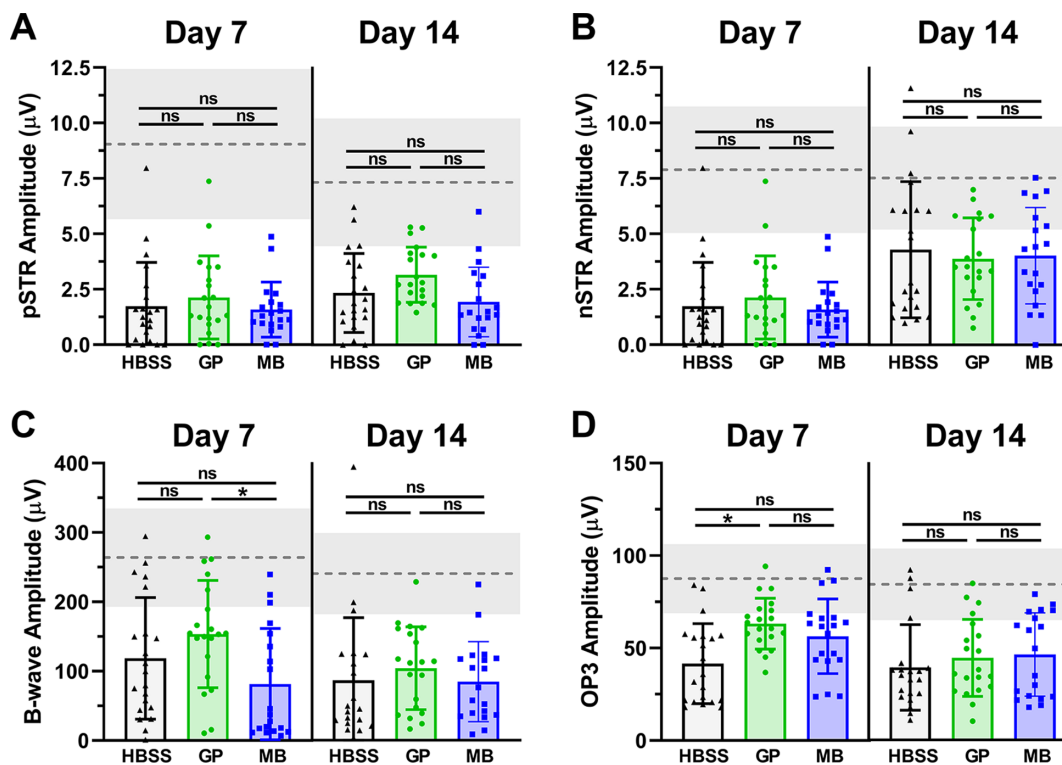


Figure 6. Retinal function is diminished in eyes with OHT and unaltered by scleral stiffening treatments. ERG functional outcomes at days 7 and 14 post-microbead injection for positive scotopic threshold (A) and negative scotopic threshold (B) were measured at $-6.0 \log \text{cd s/m}^2$, b-wave (C) was measured at a dim flash of $-3.0 \log \text{cd s/m}^2$, and OP3 (D) was measured at a bright flash of $2.1 \log \text{cd s/m}^2$. Dashed line represents mean values from normotensive controls and their corresponding standard deviations (grey band). Refer to caption of Fig. 5 for further interpretation of graphs. Significance of comparisons are listed in Supplementary Table S4. Data shown as mean ± standard deviation. ns = not significant.

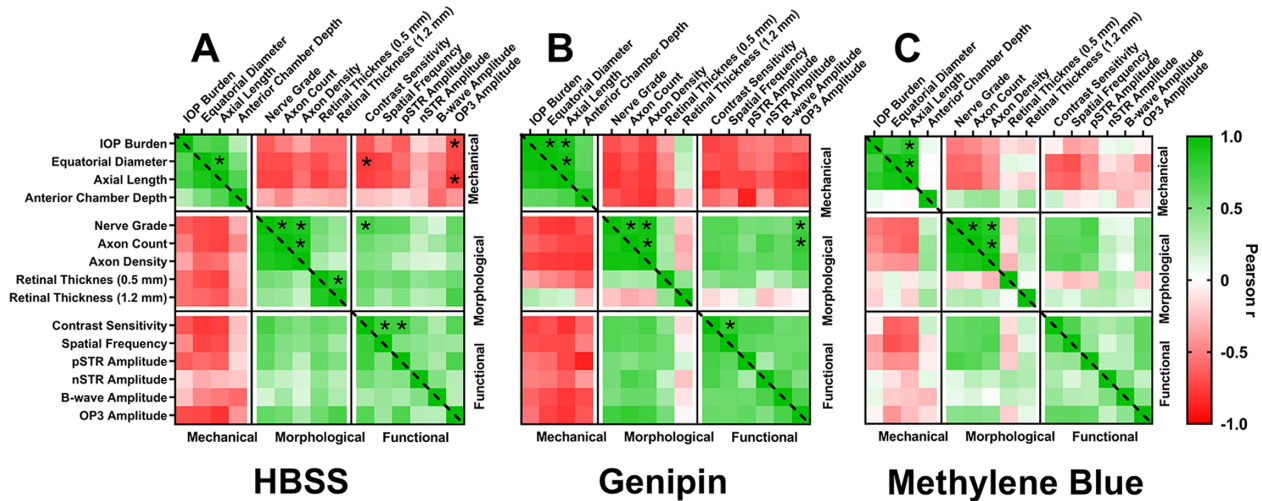


Figure 7. Overview of outcome measured for each scleral stiffening treatment group. Outcome measures in hypertensive rat eyes were organized into mechanical, morphological, and functional categories for each crosslinking treatment, and cross-correlations were evaluated. The plotted quantity is Pearson's correlation coefficient (r), a measure of the strength of association. Mechanical parameters included IOP burden, scleral strain, and eye dimensions. Morphological parameters include optic nerve cross-sectional area, axon count/density, and retinal thickness. Functional parameters include OMR and ERG data. (A) HBSS hypertensive experimental eye matrix. (B) GP hypertensive experimental eye matrix. (C) MB hypertensive experimental eye matrix. Statistical significance was calculated for null hypothesis of zero correlation ($*P < 0.05$, Bonferroni-corrected level). nSTR = negative scotopic threshold; pSTR = positive scotopic threshold.

MB treated group did not vary significantly with IOP burden for b-wave and OP3 amplitude (Supplementary Table S4) ($P > 0.05$). These results indicate that neither stiffening treatment was able to significantly preserve visual or retinal function when compared with HBSS hypertensive eyes. At the same time, these results suggest the evaluated stiffening treatments did not increase functional loss in hypertensive eyes.

Outcome Parameter Correlation Strengths Differed by Treatment

We determined correlations between the outcome measures in this study to detect associations between biomechanical, morphological, and functional outcomes within HBSS, GP, and MB treatment groups (Fig. 7). We found that functional and morphological outcomes generally correlated negatively with IOP burden. Further, the strength of the correlation was ordered GP > HBSS > MB (ranked strongest to weakest), as judged by the Pearson r magnitude averaged over all outcome measures (average r for GP = 0.63; HBSS = 0.46; MB = 0.30).

Discussion

Our goal was to assess the effects of targeted juxtaperipapillary scleral stiffening and whole posterior scleral stiffening on glaucomatous outcomes in a

microbead model of OHT in rats. To achieve this goal, we explicitly chose an unpaired experimental design, which may be counter-intuitive. However, this approach was driven by an attempt to maximize statistical power, as discussed at length in the Supplemental Material. We were successful at selectively stiffening the juxtaperipapillary sclera alone, as well as the entire posterior sclera, as confirmed by inflation testing of whole globes. Further, after induction of OHT, we observed significant changes in morphological and functional outcomes in hypertensive eyes compared with normotensive eyes, as expected (Fig. 7).

However, we did not observe significant neuroprotective effects of scleral stiffening on RGC function as measured by ERG, on visual function as measured by OMR, or on RGC axonal preservation as measured by RGC axon counts and optic nerve grading. Somewhat contrary to these findings, there was a nonsignificant trend toward the preservation of retinal thickness at 1.2 mm from the ONH in GP-treated eyes compared with HBSS treated eyes (although not in MB-treated eyes). This lack of neuroprotection occurred under both stiffening paradigms, namely juxtaperipapillary scleral stiffening around the optic nerve head vs. stiffening of the entire posterior sclera. We tested both approaches since we expected pan-scleral stiffening to increase the magnitude of dynamic effects, particularly the magnitude of IOP variations due to the ocular pulse¹³ and other time-varying features of IOP.⁵² Such IOP variations are believed to increase risk of vision loss in glaucoma⁵³ and thus we hypothesized that targeted

juxtaperipapillary stiffening would be more neuroprotective than pan-scleral stiffening. However, this was not found to be the case.

In this study we used aged rats, and it is known that the sclera stiffens with age.^{54–56} Thus, our choice to use older animals may have limited any beneficial effect of stiffening the sclera since there was presumably less “headroom” to do so in older animals. However, considering that glaucoma is more common in the elderly, we chose to use older animals since we considered them more relevant to the clinical target population. It is also noteworthy that our rate of RGC axonal loss was rapid compared to the situation in human glaucoma and some animal models of ocular hypertension, although it lay within the range of some studies using rodents.^{57–59} This suggests that RGC axons experienced significant biomechanical insult after induction of ocular hypertension, especially since we tried to carefully exclude ischemic effects as described above. It is possible that stiffening might have been more effective if the biomechanical insult was less aggressive, but this is speculative and would have to be tested in our model.

Toxicity of Crosslinking Treatments May Have Contributed to RGC Loss

We have previously evaluated the toxicity of HBSS, GP, and MB treatments in normotensive rat eyes 4 to 6 weeks after scleral stiffening.^{21,26,43} In those prior studies, we observed axonal loss owing to scleral stiffening alone, with mean RGC axon counts of 74,000, 68,000, and 46,000 for HBSS-, GP-, and MB-treated eyes, respectively.^{21,26} We also observed deficits in retinal function as measured by ERG after MB treatment in rats at 6 weeks,²⁶ but did not observe deficits in retinal function in GP-treated or HBSS-treated eyes at 4 weeks.²¹ For the MB photocrosslinking procedure, it was found previously that light alone did not cause significant morphological changes, and that such changes were observed only in the presence of both MB and light.²⁶ This modest RGC axonal loss owing to GP, and the more significant loss owing to MB, must be considered when interpreting our results. Interestingly, despite the previous finding that the MB photocrosslinking treatment induced more significant damage than did the GP treatment, in this study, we did not observe appreciable differences in axon loss between cohorts at low IOP burdens (i.e., where the effect of treatment toxicity would dominate effect of induced hypertensive damage).^{21,26} It is possible there were neuroprotective effects of scleral stiffening that were counteracted by the toxicity of the

stiffening treatment itself. Thus, the development of alternative scleral stiffening approaches that have less inherent RGC toxicity would be an important aspect of future research in this area. Although collateral crosslinking treatment toxicity may explain the observations in this study, it is noted that the desired tissue mechanical changes may themselves also contributed to morphological changes and functional deficits as well. However, it is difficult to disentangle these two possible factors without further studies.

Variability of the Microbead Model Complicates Interpretation of These Results

A significant drawback in our study was the highly variable outcomes in the microbead model of OHT in Brown Norway rats, specifically interanimal variation in the time course and magnitude of IOP elevation, as reflected in the wide range of IOP burdens. This variation led to significant scatter in our outcome measures, even when considering IOP burden as a covariate, and decreased the power to detect differences between scleral stiffening treatments.

Additionally, the microbead model of OHT caused rapid, transient pressure elevations, which is not typical of the IOP history seen in patients with open-angle glaucoma.^{30,52,54} Therefore, the biomechanical insult seen in our study may be more severe than would be observed clinically. That being said, we excluded eyes that experienced excessive insult attributed to artifactually high IOP that could cause ischemia, as discussed in the Supplementary Material and in our prior publication.⁴² Furthermore, our 14-day study duration was far shorter than clinical OHT, and adaptive responses such as collagen remodeling in the sclera may not have fully manifested. In summary, future studies should use OHT models with lower variability and that more closely mimic the glaucomatous eye in human clinical experience, in which IOP is continuously monitored and controlled.^{54,55}

The Posterior Sclera Was Successfully Stiffened With Both Targeted and Nontargeted Treatments

Scleral strain measured post mortem with whole globe inflation tests confirmed successful targeted juxtaperipapillary scleral stiffening with MB and posterior scleral stiffening with GP (Fig. 2B). Strain, rather than a direct assessment of crosslinking, was assessed in this study as a functional outcome, motivated by a previous study showing a decrease in strain in the optic nerve region with scleral stiffening.¹¹ Additionally,

practical limitations in the ability to quantify crosslinking simultaneously with this functional outcome informed the selection of strain as the mechanical measurement of choice.

We observed increasing strain values (decreased stiffness) with increasing IOP burden in HBSS eyes, indicating weakening of the sclera under hypertensive conditions in this study (Supplementary Fig. S7). These effects are likely due to the fairly short time scale of this study, and are consistent with early scleral remodeling, as shown in a number of studies.^{56–60} For example, Burgoyne et al.⁶¹ showed early scleral biomechanical softening after OHT in nonhuman primates, and Korneva et al.⁶² observed a similar effect in the peripapillary sclera of mice. The observed increase in hypertensive eye size with increased IOP burden (Fig. 4) is also indicative of early scleral remodeling. This increase in globe size differs from the case of human adult glaucoma, where an elevated IOP is not known to lead to ocular enlargement. However, other rodent models of OHT have observed similar findings of OHT-induced globe enlargement.^{12,32}

In addition to quantification of strain, strain maps were qualitatively assessed to detect whether there were significant differences between quadrants. No differences by quadrant were observed. All quadrants were, therefore, averaged to produce a less noisy overall strain measurement in the juxtaperipapillary and peripheral regions. A limitation of our strain measurement technique is that it only interrogated the outer scleral surface and therefore cannot explicitly determine through scleral stiffening effects. Thus, an implicit assumption is that the superficial layer's mechanical properties would reflect those of the underlying layers; we feel that this assumption is reasonable since the scleral displacement measured by DIC will depend on all scleral layers. Another possible limitation of the whole globe inflation testing method is the use of mineral oil as a pressurizing fluid. Theoretically, the use of oil rather than buffer solution could alter the acute hydration state of the tissue, thus affecting the strain measurements. However, all eyes underwent the same inflation testing procedure using mineral oil, and thus we expect that strain differences between treatments could be detected reliably. Finally, we did not assess whether stiffening changed over the 14 day course of our study. However, in a previous study considering genipin-induced stiffening,²⁰ scleral stiffening at 1 day post-genipin was similar that seen at 28 days. In that paper, the average reduction in scleral strain was 58.6%, which may be compared to a similar computation in the present work (based on data in Supplemental Table S6), giving a strain reduction in the juxtaperipapillary region of 63% for GP eyes and 62% for MB eyes. These comparable values at 3 time points suggest that

scleral stiffening was relatively sustained over the entire duration of the present study.

Other investigators have considered noncrosslinking mechanisms to modulate scleral properties as a neuroprotective strategy. Quigley et al.⁶³ showed that the angiotensin II receptor blocker, losartan, affected scleral remodeling and was neuroprotective in a mouse model of glaucoma. Later, Hazlewood et al.⁶⁴ obtained a similar result using a different receptor blocker. The mechanisms of these blockers are undoubtedly complex, but may be mediated through the modulation of scleral properties. It is conceivable that such modulation must be sustained over time to confer neuroprotection, rather than a one-time cross-linking treatment. However, we note that scleral stiffening was maintained throughout the duration of our study, so this putative explanation requires further investigation.

Comparison of Structural and Functional Outcomes

There were no observed differences between RGC function (ERG) or visual function (OMR) between HBSS and the two treatment groups (Table). Functional outcomes are perhaps most relevant to clinical translation irrespective of morphological changes.

Previously, it has been shown that axon loss precedes retinal thinning, which may explain the relatively large deficit in axon count observed compared with the more minor retinal thinning in our study.⁶⁵ The loss of retinal thickness in MB eyes at 0.5 mm distance from the ONH may be due to hypertension-linked RGC loss and to localized toxicity of the photocrosslinking procedure. Recall that the region 0.5 to 1.0 mm from the ONH was selectively targeted for treatment in these eyes, likely inducing more damage at 0.5 mm than at 1.2 mm.

It should be noted that our OCT measurements were of TRT because we could not confidently resolve the retinal nerve fiber layer in our imaging after microbead injection. However, we suspect our measurements of TRT at both measurement locations were likely related to retinal nerve fiber layer thinning, because we also observed significant loss of RGC axons (Figs. 4C–F) and RGC function (Figs. 6A–D) in HBSS hypertensive experimental eyes compared with normotensive controls. One limitation of this study was our choice to use two radial b-scans instead of a circular b-scan as described previously.⁶⁶ Although our current protocol did average retinal thickness measurements from all quadrants, having more data points would have provided more accuracy and should be implemented in future studies.

Outcome Parameter Correlation Strengths Differed by Treatment

Individual correlations between outcome measures and IOP burden were generally not statistically significant (Fig. 7). It is useful to measure correlations between outcome measures and IOP burden to assess the impact of IOP burden on outcome measures. Generally, outcome measures decreased with increasing IOP burden (negative correlations). Although not statistically significant for individual correlations, we observed strongest Pearson r correlations in GP, followed by HBSS, followed by MB. These findings suggest that outcome measures in GP-treated eyes were most sensitive to IOP burden, whereas those of the MB eyes were least sensitive. Owing to the potential for confounding variables in the microbead model of OHT, we cannot conclude that these associations reflect differences in treatment effects. However, they are interesting for the purposes of understanding associations across multiple outcome parameters, which have been treated more extensively individually in this study.

Key Differences Exist Between This Study and a Similar Previous Study

It is of interest to compare our results with those of the related study of Kimball et al.¹² (Supplementary Table S1). Kimball et al. examined the effect of scleral stiffening using a different crosslinking agent, glycer-aldehyde, in OHT mice and found that scleral stiffening made adverse effects of glaucoma worse, as determined by RGC axon counts. This contrasts with the findings of our study, in which scleral stiffening did not appear to provide neuroprotection, but also did not show evidence of making glaucomatous damage worse.

There are a number of differences between our study and the one performed by Kimball et al. First, whereas Kimball et al. stiffened the sclera throughout the eye in a nontargeted manner, our approach involved stiffening designed to target just the posterior sclera (with a retrobulbar injection of GP into the muscle cone²⁰) or, even more focused, just the juxtaperipapillary sclera (with photocrosslinked MB). Additionally, Kimball et al. observed an 18% axon loss in their control microbead group, whereas we observed a greater degree of axon loss in our HBSS control animals (55%). We believe the degree of axon loss observed in the current study should be sufficient to resolve any neuroprotective effects of stiffening. Further, Kimball et al. stiffened the sclera using glycer-aldehyde in 100 mM sodium phosphate (Na_3PO_4), the latter having an osmolarity of 400 mOsm.¹² After addition of 500 mM glycer-aldehyde, the solution's final osmolarity would

have been 900 mOsm, which exceeds the physiological osmolarity of 285 to 295 mOsm.⁶⁷ With this finding in mind, we chose to examine two biocompatible stiffening agents with osmolarities within the physiological osmolarity range to reduce potential toxicity. Another difference is that Kimball et al. did not assess functional outcomes in stiffened OHT eyes. To provide a more complete characterization, we chose to include functional outcomes encompassing visual function (OMR), retinal function (ERG), and retinal thickness (OCT), thus better clarifying the effects of scleral stiffening on clinically relevant outcomes. It is important to note that we did not find increased functional or morphological damage in whole posterior sclera stiffened hypertensive eyes in any outcome measure. Yet another difference between our study and that of Kimball et al. is the use of adult rats (aged 8–10 months), which is older (in terms of lifespan) than the 2-month-old mice used by Kimball et al.¹² Age is a well-established risk factor for glaucomatous optic neuropathy, for example,⁶⁸ and it would be interesting to repeat these experiments in younger rats (or older mice).

There Are Notable Limitations in the Present Study

Before the start of this study, the tonometer was calibrated in untreated normotensive and hypertensive eyes (see Supplementary Material), but was not calibrated in HBSS, GP, or MB normotensive eyes. We previously found no significant differences in tonometric measurement of IOP when comparing GP, HBSS, and naïve eyes.²¹ We did not check this possibility in MB-treated eyes, but find it unlikely that there would be an effect on IOP measurement since there was no effect on IOP in GP-treated eyes.

Our ERG-based exclusion criterion developed by Hannon et al.⁴² used one-time ERG measurement to infer ischemic damage when histological changes were not apparent. There are retinal ischemia–reperfusion studies, such as⁶⁹ that examine retinal histology after short-term exposure to elevated IOP. However, typically a longer duration of ischemia is necessary to obtain histological changes.⁷⁰ Thus, we chose to evaluate retinal function using an *in vivo* measurement since this permitted post-mortem analysis of eyes (in our case, scleral strain measurements).

A limitation of our experimental approaches is that tissues other than the sclera could be stiffened due to “off-target” action of the cross-linker. This was an unavoidable aspect of our protocol, and we speculate that such “off-target” stiffening could possibly affect the walls of retinal and/or choroidal vessels, extraocular muscles, and/or the optic nerve sheath. Cross-linking of the optic nerve sheath and/or extraocular

muscles would likely be more severe in the case of genipin retrobulbar injection, since the transpupillary light delivery was more localized and light intensity attenuation with position would somewhat limit the posterior extent of any stiffening. On the other hand, cross-linking of choroidal vessels could be more significant with the light-activated methylene blue protocol, since light intensity would be only slightly attenuated at the level of the choroid.²⁶ Sun et al. specifically examined the effects of choroidal vessel wall cross-linking, observing that it did not affect vascular flow density in monkeys, as determined by OCT-angiography.⁸⁰ This is generally consistent with our observations: we did not see any changes in retinal function from stiffening alone,²¹ which suggests that any changes to the vasculature due to cross-linking of the vessel wall did not significantly impact outer retinal function. Stiffening of the optic nerve sheath could affect optic nerve head biomechanical loading during globe rotation,^{81–84} which of course will depend on extraocular muscle function. Unfortunately, measurement of globe rotation in rodents requires specialized equipment and techniques^{85,86} and was beyond the scope of this work, and thus we cannot explicitly comment on whether optic nerve sheath stiffening effects were significant or not in our experiments. Further careful exploration of such potential “off-target” effects would be required if this therapy were to be translated into the clinic.

Another limitation is that we measured total retinal thickness rather than RNFL thickness in OCT scans to assess RGC axonal loss. We chose this approach because limitations in the resolution of our OCT system and occasional optical aberrations caused by the microbeads themselves made reliable determination of RNFL thickness challenging. Total retinal thickness was a more repeatable measurement, although could have been affected by non-RNFL changes in the retina.

Finally, we know that the sclera remodels (in a non-monotonic manner) after induction of ocular hypertension.^{70,71} It is possible that scleral stiffening could interact with this scleral remodeling process in a complex way. If cross-linking were to be considered as a clinical treatment, further studies of such an interaction would be required since time scales for IOP elevation and scleral remodeling are typically slower in human subjects vs. the relatively rapid effects in our rat model of ocular hypertension.

Conclusions

The treatment of the eye with GP or with MB in combination with laser exposure effectively increased

scleral stiffness. However, neither targeted juxtapapillary nor nontargeted posterior scleral stiffening by these methods preserved morphological and functional outcomes in an ocular hypertensive rat model. Although this study did not show neuroprotective effects of scleral stiffening in the glaucomatous eye, it did not rule out the possibility that this approach might still have merit. The interpretation of our results is hindered by the high variability and other drawbacks of the microbead model of OHT, as well as evidence of inherent retinal toxicity of the scleral stiffening treatment. Further research is needed to investigate the impact of scleral stiffening on glaucomatous damage, but should be conducted using less toxic scleral stiffening treatments and a better OHT model.

Acknowledgments

The authors thank Richard Schaefer for his expertise in optics/microscopy, Laura O’Farrell, Richard Noel, and Sandra Meyer for veterinary expertise, and Donna Bondy for administrative support.

Supported by NIH R01 EY025286 (CRE and MRP) and 5T32 EY007092-32 (BGH), Department of Veterans Affairs Rehab R&D Service Career Development Awards to AJF (CDA-2; RX002342) and Senior Research Career Scientist Award to MTP (RX003134), the Georgia Research Alliance (CRE), and the Centers for Disease Control and Oak Ridge Institute for Science and Education (BGG).

Disclosure: **B.G. Gerberich**, None; **B.G. Hannon**, None; **D.M. Brown**, None; **A.T. Read**, None; **M.D. Ritch**, None; **E. Schrader Echeverri**, None; **L. Nichols**, None; **C. Potnis**, None; **S. Sridhar**, None; **M.G. Toothman**, None; **S.A. Schwaner**, None; **E.J. Winger**, None; **H. Huang**, None; **G.S. Gershon**, None; **A.J. Feola**, None; **M.T. Pardue**, None; **M.R. Prausnitz**, None; **C.R. Ethier**, None

* BGG and BGH contributed equally to this work.

References

1. Quigley HA, Broman AT. The number of people with glaucoma worldwide in 2010 and 2020. *Br J Ophthalmol*. 2006;90:262–267.
2. Quigley HA, Addicks EM, Green WR, Maumenee AE. Optic nerve damage in human glaucoma. II. The site of injury and susceptibility to damage. *Arch Ophthalmol*. 1981;99:635–649.

3. Weinreb RN, Khaw PT. Primary open-angle glaucoma. *Lancet*. 2004;363:1711–1720.
4. Klein BE, Klein R, Sponsel WE, et al. Prevalence of glaucoma. The Beaver Dam Eye Study. *Ophthalmology*. 1992;99:1499–1504.
5. Weinreb RN, Aung T, Medeiros FA. The pathophysiology and treatment of glaucoma: a review. *JAMA*. 2014;311:1901–1911.
6. Heijl A, Leske MC, Bengtsson B, et al. Reduction of intraocular pressure and glaucoma progression: results from the Early Manifest Glaucoma Trial. *Arch Ophthalmol*. 2002;120:1268–1279.
7. Gurwitz JH, Yeomans SM, Glynn RJ, Lewis BE, Levin R, Avorn J. Patient noncompliance in the managed care setting. The case of medical therapy for glaucoma. *Med Care*. 1998;36:357–369.
8. Campbell IC, Coudrillier B, Ethier CR. Biomechanics of the posterior eye: a critical role in health and disease. *J Biomech Eng*. 2014;136:021005.
9. Sigal IA, Flanagan JG, Ethier CR. Factors influencing optic nerve head biomechanics. *Invest Ophthalmol Vis Sci*. 2005;46:4189–4199.
10. Sigal IA, Flanagan JG, Tertinegg I, Ethier CR. Finite element modeling of optic nerve head biomechanics. *Invest Ophthalmol Vis Sci*. 2004;45:4378–4387.
11. Coudrillier B, Campbell IC, Read AT, et al. Effects of peripapillary scleral stiffening on the deformation of the lamina cribrosa. *Invest Ophthalmol Vis Sci*. 2016;57:2666–2677.
12. Kimball EC, Nguyen C, Steinhart MR, et al. Experimental scleral cross-linking increases glaucoma damage in a mouse model. *Exp Eye Res*. 2014;128:129–140.
13. Clayson K, Pan X, Pavlatos E, et al. Corneoscleral stiffening increases IOP spike magnitudes during rapid microvolumetric change in the eye. *Exp Eye Res*. 2017;165:29–34.
14. Asrani S, Zeimer R, Wilensky J, Gieser D, Vitale S, Lindenmuth K. Large diurnal fluctuations in intraocular pressure are an independent risk factor in patients with glaucoma. *J Glaucoma*. 2000;9:134–142.
15. Huang LL, Sung HW, Tsai CC, Huang DM. Biocompatibility study of a biological tissue fixed with a naturally occurring crosslinking reagent. *J Biomed Mater Res*. 1998;42:568–576.
16. Avila MY, Navia JL. Effect of genipin collagen crosslinking on porcine corneas. *J Cataract Refract Surg*. 2010;36:659–664.
17. Liu TX, Wang Z. Biomechanics of sclera crosslinked using genipin in rabbit. *Int J Ophthalmol*. 2017;10:355–360.
18. Song W, Tang Y, Qiao J, et al. The comparative safety of genipin versus UVA-riboflavin crosslinking of rabbit corneas. *Mol Vis*. 2017;23:504–513.
19. Campbell IC, Hannon BG, Read AT, Sherwood JM, Schwaner SA, Ethier CR. Quantification of the efficacy of collagen cross-linking agents to induce stiffening of rat sclera. *J R Soc Interface*. 2017;14:20170014.
20. Hannon BG, Schwaner SA, Boazak EM, et al. Sustained scleral stiffening in rats after a single genipin treatment. *J R Soc Interface*. 2019;16:20190427.
21. Hannon BG, Luna C, Feola AJ, et al. Assessment of visual and retinal function following in vivo genipin-induced scleral crosslinking. *Transl Vis Sci Technol*. 2020;9:8.
22. Johnson EC, Deppmeier LM, Wentzien SK, Hsu I, Morrison JC. Chronology of optic nerve head and retinal responses to elevated intraocular pressure. *Invest Ophthalmol Vis Sci*. 2000;41:431–442.
23. Guo L, Moss SE, Alexander RA, Ali RR, Fitzke FW, Cordeiro MF. Retinal ganglion cell apoptosis in glaucoma is related to intraocular pressure and IOP-induced effects on extracellular matrix. *Invest Ophthalmol Vis Sci*. 2005;46:175–182.
24. Morrison JC, Cepurna Ying Guo WO, Johnson EC. Pathophysiology of human glaucomatous optic nerve damage: insights from rodent models of glaucoma. *Exp Eye Res*. 2011;93:156–164.
25. Jia L, Cepurna WO, Johnson EC, Morrison JC. Effect of general anesthetics on IOP in rats with experimental aqueous outflow obstruction. *Invest Ophthalmol Vis Sci*. 2000;41:3415–3419.
26. Gerberich BG, Hannon BG, Hejri A, et al. Transpupillary collagen photocrosslinking for targeted modulation of ocular biomechanics. *Biomaterials*. 2021;271:120735.
27. Lozano DC, Twa MD. Development of a rat schematic eye from in vivo biometry and the correction of lateral magnification in SD-OCT imaging. *Invest Ophthalmol Vis Sci*. 2013;54:6446–6455.
28. Fazio MA, Grytz R, Bruno L, et al. Regional variations in mechanical strain in the posterior human sclera. *Invest Ophthalmol Vis Sci*. 2012;53:5326–5333.
29. Cone-Kimball E, Nguyen C, Oglesby EN, Pease ME, Steinhart MR, Quigley HA. Scleral structural alterations associated with chronic experimental intraocular pressure elevation in mice. *Mol Vis*. 2013;19:2023–2039.
30. Bunker S, Holeniewska J, Vijay S, et al. Experimental glaucoma induced by ocular injection of magnetic microspheres. *J Vis Exp*. 2015.
31. Samsel PA, Kisiswa L, Erichsen JT, Cross SD, Morgan JE. A novel method for the induction

- of experimental glaucoma using magnetic microspheres. *Invest Ophthalmol Vis Sci.* 2011;52:1671–1675.
32. Frankfort BJ, Khan AK, Tse DY, et al. Elevated intraocular pressure causes inner retinal dysfunction before cell loss in a mouse model of experimental glaucoma. *Invest Ophthalmol Vis Sci.* 2013;54:762–770.
 33. Sappington RM, Carlson BJ, Crish SD, Calkins DJ. The microbead occlusion model: a paradigm for induced ocular hypertension in rats and mice. *Invest Ophthalmol Vis Sci.* 2010;51:207–216.
 34. Mabuchi F, Aihara M, Mackey MR, Lindsey JD, Weinreb RN. Optic nerve damage in experimental mouse ocular hypertension. *Invest Ophthalmol Vis Sci.* 2003;44:4321–4330.
 35. Chen H, Zhao Y, Liu M, et al. Progressive degeneration of retinal and superior collicular functions in mice with sustained ocular hypertension. *Invest Ophthalmol Vis Sci.* 2015;56:1971–1984.
 36. Bui BV, Edmunds B, Cioffi GA, Fortune B. The gradient of retinal functional changes during acute intraocular pressure elevation. *Invest Ophthalmol Vis Sci.* 2005;46:202–213.
 37. Bui BV, Fortune B. Ganglion cell contributions to the rat full-field electroretinogram. *J Physiol.* 2004;555:153–173.
 38. Bui BV, He Z, Vingrys AJ, Nguyen CT, Wong VH, Fortune B. Using the electroretinogram to understand how intraocular pressure elevation affects the rat retina. *J Ophthalmol.* 2013;2013:262467.
 39. Grillo SL, Montgomery CL, Johnson HM, Koulen P. Quantification of changes in visual function during disease development in a mouse model of pigmentary glaucoma. *J Glaucoma.* 2018;27:828–841.
 40. Douglas RM, Alam NM, Silver BD, McGill TJ, Tschetter WW, Prusky GT. Independent visual threshold measurements in the two eyes of freely moving rats and mice using a virtual-reality optokinetic system. *Vis Neurosci.* 2005;22:677–684.
 41. Prusky GT, Alam NM, Beekman S, Douglas RM. Rapid quantification of adult and developing mouse spatial vision using a virtual optomotor system. *Invest Ophthalmol Vis Sci.* 2004;45:4611–4616.
 42. Hannon BG, Feola AJ, Gerberich BG, et al. Using retinal function to define ischemic exclusion criteria for animal models of glaucoma. *Exp Eye Res.* 2020;202:108354.
 43. Hannon BG. Stiffening the posterior rat sclera to provide neuroprotection in glaucoma. *BioEngineering.* Atlanta: Georgia Institute of Technology; 2020. Available at: <https://smartech.gatech.edu/handle/1853/63648>. Accessed April 6, 2022.
 44. Matsumoto CS, Shinoda K, Nakatsuka K. High correlation of scotopic and photopic electroretinogram components with severity of central retinal artery occlusion. *Clin Ophthalmol.* 2011;5:115–121.
 45. Zhao Y, Yu B, Xiang YH, et al. Changes in retinal morphology, electroretinogram and visual behavior after transient global ischemia in adult rats. *PLoS One.* 2013;8:e65555.
 46. Feola AJ, Fu J, Allen R, et al. Menopause exacerbates visual dysfunction in experimental glaucoma. *Exp Eye Res.* 2019;186:107706.
 47. Ritch MD, Hannon BG, Read AT, et al. AxoNet: a deep learning-based tool to count retinal ganglion cell axons. *arXiv e-prints*; 2019.
 48. Ritch MD, Hannon BG, Read AT, et al. AxoNet: A deep learning-based tool to count retinal ganglion cell axons. *Sci Rep.* 2020;10:8034.
 49. Jia L, Cepurna WO, Johnson EC, Morrison JC. Patterns of intraocular pressure elevation after aqueous humor outflow obstruction in rats. *Invest Ophthalmol Vis Sci.* 2000;41:1380–1385.
 50. Chauhan BC, Levatte TL, Garnier KL, et al. Semi-quantitative optic nerve grading scheme for determining axonal loss in experimental optic neuropathy. *Invest Ophthalmol Vis Sci.* 2006;47:634–640.
 51. Schneider CA, Rasband WS, Eliceiri KW. NIH Image to ImageJ: 25 years of image analysis. *Nat Methods.* 2012;9:671–675.
 52. Smedowski A, Pietrucha-Dutczak M, Kaarniranta K, Lewin-Kowalik J. A rat experimental model of glaucoma incorporating rapid-onset elevation of intraocular pressure. *Sci Rep.* 2014;4:5910.
 53. Urcola JH, Hernandez M, Vecino E. Three experimental glaucoma models in rats: comparison of the effects of intraocular pressure elevation on retinal ganglion cell size and death. *Exp Eye Res.* 2006;83:429–437.
 54. Ficarrotta KR, Mohamed YH, Passaglia CL. Experimental glaucoma model with controllable intraocular pressure history. *Sci Rep.* 2020;10:126.
 55. Morrison JC, Cepurna WO, Tehrani S, et al. A period of controlled elevation of IOP (CEI) produces the specific gene expression responses and focal injury pattern of experimental rat glaucoma. *Invest Ophthalmol Vis Sci.* 2016;57:6700–6711.
 56. Bellezza AJ, Rintalan CJ, Thompson HW, Downs JC, Hart RT, Burgoyne CF. Deformation of the lamina cribrosa and anterior scleral canal wall in early experimental glaucoma. *Invest Ophthalmol Vis Sci.* 2003;44:623–637.
 57. Burgoyne CF, Quigley HA, Thompson HW, Vitale S, Varma R. Early changes in optic disc compliance

- and surface position in experimental glaucoma. *Ophthalmology*. 1995;102:1800–1809.
58. Yang H, Ren R, Lockwood H, et al. The connective tissue components of optic nerve head cupping in monkey experimental glaucoma part 1: global change. *Invest Ophthalmol Vis Sci*. 2015;56:7661–7678.
 59. Ivers KM, Yang H, Gardiner SK, et al. In vivo detection of laminar and peripapillary scleral hypercompliance in early monkey experimental glaucoma. *Invest Ophthalmol Vis Sci*. 2016;57:OCT388–OCT403.
 60. Girard MJ, Suh JK, Bottlang M, Burgoyne CF, Downs JC. Biomechanical changes in the sclera of monkey eyes exposed to chronic IOP elevations. *Invest Ophthalmol Vis Sci*. 2011;52:5656–5669.
 61. Fazio MA, Girard MJA, Lee W, Morris JS, Burgoyne CF, Downs JC. The relationship between scleral strain change and differential cumulative intraocular pressure exposure in the nonhuman primate chronic ocular hypertension model. *Invest Ophthalmol Vis Sci*. 2019;60:4141–4150.
 62. Korneva A, Kimball EC, Jefferys JL, Quigley HA, Nguyen TD. Biomechanics of the optic nerve head and peripapillary sclera in a mouse model of glaucoma. *J R Soc Interface*. 2020;17:20200708.
 63. Quigley HA, Pitha IF, Welsbie DS, et al. Losartan treatment protects retinal ganglion cells and alters scleral remodeling in experimental glaucoma. *PLoS One*. 2015;10:e0141137.
 64. Hazlewood RJ, Kuchtey J, Wu HJ, Kuchtey RW. Telmisartan reduces axon degeneration in mice with experimental glaucoma. *Invest Ophthalmol Vis Sci*. 2020;61:51.
 65. Calkins DJ. Critical pathogenic events underlying progression of neurodegeneration in glaucoma. *Prog Retin Eye Res*. 2012;31:702–719.
 66. Lakshmanan Y, Wong FSY, Zuo B, Bui BV, Chan HH. Longitudinal outcomes of circumlimbal suture model-induced chronic ocular hypertension in Sprague-Dawley albino rats. *Graefes Arch Clin Exp Ophthalmol*. 2020;258(12):2715–2728.
 67. Fox SI. *Human physiology*, 12th ed. New York: McGraw-Hill; 2011.
 68. Guedes G, Tsai JC, Loewen NA. Glaucoma and aging. *Curr Aging Sci*. 2011;4:110–117.
 69. Adachi M, Takahashi K, Nishikawa M, Miki H, Uyama M. High intraocular pressure-induced ischemia and reperfusion injury in the optic nerve and retina in rats. *Graefes Arch Clin Exp Ophthalmol*. 1996;234:445–451.
 70. Selles-Navarro I, Villegas-Perez MP, Salvador-Silva M, Ruiz-Gomez JM, Vidal-Sanz M. Retinal ganglion cell death after different transient periods of pressure-induced ischemia and survival intervals. A quantitative in vivo study. *Invest Ophthalmol Vis Sci*. 1996;37:2002–2014.
 71. Korneva A, Kimball EC, Jefferys JL, Quigley HA, Nguyen TD. Biomechanics of the optic nerve head and peripapillary sclera in a mouse model of glaucoma. *J R Soc Interface*. 2020;17:20200708.
 72. Quigley HA, Pitha IF, Welsbie DS, et al. Losartan Treatment Protects Retinal Ganglion Cells and Alters Scleral Remodeling in Experimental Glaucoma. *PLoS One*. 2015;10:e0141137.
 73. Hazlewood RJ, Kuchtey J, Wu HJ, Kuchtey RW. Telmisartan Reduces Axon Degeneration in Mice With Experimental Glaucoma. *Invest Ophthalmol Vis Sci*. 2020;61:51.
 74. Calkins DJ. Critical pathogenic events underlying progression of neurodegeneration in glaucoma. *Prog Retin Eye Res*. 2012;31:702–719.
 75. Lakshmanan Y, Wong FSY, Zuo B, Bui BV, Chan HH. Longitudinal outcomes of circumlimbal suture model-induced chronic ocular hypertension in Sprague-Dawley albino rats. *Graefes Arch Clin Exp Ophthalmol*. 2020.
 76. Fox SI. *Human physiology*. 12nd ed. New York: McGraw-Hill; 2011.
 77. Guedes G, Tsai JC, Loewen NA. Glaucoma and aging. *Curr Aging Sci*. 2011;4:110–117.
 78. Adachi M, Takahashi K, Nishikawa M, Miki H, Uyama M. High intraocular pressure-induced ischemia and reperfusion injury in the optic nerve and retina in rats. *Graefes Arch Clin Exp Ophthalmol*. 1996;234:445–451.
 79. Selles-Navarro I, Villegas-Perez MP, Salvador-Silva M, Ruiz-Gomez JM, Vidal-Sanz M. Retinal ganglion cell death after different transient periods of pressure-induced ischemia and survival intervals. A quantitative in vivo study. *Invest Ophthalmol Vis Sci*. 1996;37:2002–2014.
 80. Sun M, Zhang F, Ouyang B, et al. Study of retina and choroid biological parameters of rhesus monkeys eyes on scleral collagen cross-linking by riboflavin and ultraviolet A. *PLoS One*. 2018;13:e0192718.
 81. Wang X, Beotra MR, Tun TA, et al. In Vivo 3-Dimensional Strain Mapping Confirms Large Optic Nerve Head Deformations Following Horizontal Eye Movements. *Invest Ophthalmol Vis Sci*. 2016;57:5825–5833.
 82. Wang X, Fisher LK, Milea D, Jonas JB, Girard MJ. Predictions of Optic Nerve Traction Forces and Peripapillary Tissue Stresses Following Horizontal Eye Movements. *Invest Ophthalmol Vis Sci*. 2017;58:2044–2053.

83. Wang X, Rumpel H, Lim WE, et al. Finite Element Analysis Predicts Large Optic Nerve Head Strains During Horizontal Eye Movements. *Invest Ophthalmol Vis Sci.* 2016;57:2452–2462.
84. Chang MY, Shin A, Park J, et al. Deformation of Optic Nerve Head and Peripapillary Tissues by Horizontal Duction. *Am J Ophthalmol.* 2017;174:85–94.
85. Stahl JS. Using eye movements to assess brain function in mice. *Vision Res.* 2004;44:3401–851, 3410.
86. Stahl JS, van Alphen AM, De Zeeuw CI. A comparison of video and magnetic search coil recordings of mouse eye movements. *J Neurosci Methods.* 2000;99:101–110.